Influence of the sample morphology on total reflection X-ray fluorescence analysis

C. Horntrich, F. Meirer, C. Streli, and P. Kregsamer
Vienna University of Technology, Atominstitut, Stadionallee 2, 1020 Vienna, Austria

G. Pepponi
FBK-irst, via Sommarive 18, 38050 Povo (Trento), Italy

N. Zoeger and P. Wobrauschek
Vienna University of Technology, Atominstitut, Stadionallee 2, 1020 Vienna, Austria

(Received 30 September 2008; accepted 20 January 2009)

Total reflection X-ray fluorescence analysis (TXRF) is a method for qualitative and quantitative analysis of trace elements. In general TXRF is known to allow for linear calibration typically using an internal standard for quantification. For small sample amounts (low ng region) the thin film approximation is valid neglecting absorption effects of the exciting and the detected radiation. However, for higher total amounts of samples deviations from the linear relation between fluorescence intensity and sample amount have been observed. The topic of the presented work is an investigation of the parameters influencing the absorption phenomenon. Samples with different total amounts of arsenic have been prepared to determine the upper limit of sample mass where the linear relation between fluorescence intensity and sample amount is no longer guaranteed. It was found that the relation between fluorescence intensity and sample amount is linear up to ~100 ng arsenic. A simulation model was developed to calculate the influence of the absorption effects. Even though the results of the simulations are not satisfying yet it could be shown that one of the key parameters for the absorption effect is the density of the investigated element in the dried residues. © *2009 International Centre for Diffraction Data.* [DOI: 10.1154/1.3131804]

Key words: TXRF, absorption effects, quantification

I. INTRODUCTION

Total reflection X-ray fluorescence analysis (TXRF) offers a nondestructive qualitative and quantitative analysis of trace elements and is extremely surface-sensitive. With TXRF the analysis of very small sample amounts is possible and the detection limits are in the pg-range (if the excitation source is an X-ray tube) [Wobrauschek *et al.*, 1991; Wobrauschek *et al.*, 1992; Ladisich *et al.*, 1993; Kregsamer *et al.*, 2001; Stoev and Sakurai, 1999; Pahlke, 2003; Pahlke *et al.*, 2001; Fabry and Pahlke, 2002; Klockenkämper, 1996]. In TXRF, absorption effects concerning exciting and detected radiation are usually disregarded. This is justified because mostly small sample amounts are used. The thin film approximation in particular assumes a very thin sample and therefore differential absorption for photons with different energies can be ignored. Furthermore the elements in the sample are assumed to be homogeneously distributed. Hence the loss of the fluorescence signal due to absorption of the primary beam equally affects all elements and quantification by using an internal standard is justified (Prange and Schwenke, 1992; Wobrauschek, 2007). For higher total amounts of samples deviations from the linear relation between fluorescence intensity and sample amount have been observed (Hellin *et al.*, 2004b; Hellin *et al.*, 2004a; Hellin *et al.*, 2005). An investigation of the parameters influencing the absorption phenomenon is the content of the presented work. A simulation model was developed to calculate the influence of the absorption effects. Samples with different total amounts of arsenic were prepared to determine the upper limit of sample mass where the linear relation between fluorescence intensity and sample amount is no longer guaranteed. Furthermore the sample shapes on different reflector materials, as a result of drying, were investigated (by analyses with a confocal white light microscope) as well as the influence of the sample geometry on absorption effects.

II. EXPERIMENTAL

A. Preparation of the samples

In this study we used a Si wafer, an acrylic glass reflector, and quartz reflectors. They were measured with TXRF (ATOMIKA EXTRA-IIA system, for experimental setup see "analytical procedure") and no contaminations were detected. For the linearity test different amounts of arsenic (4, 7, 9, 20, 40, 71, 100, 179, 300, 362, and 503 ng) were put on several quartz reflectors. An arsenic standard solution was used ($H3AsO_4$ in HNO_3, contains 1000 mg/L arsenic, Producer: Merck). Using this standard solution a dilution series with different concentrations of arsenic was prepared. One μL of a specific solution of the dilution series was put on each reflector. The reflectors were weighed to determine the effective arsenic amount (balance: SARTORIUS R300S, error: $\pm$0.1 mg) and afterwards the samples were dried on a heating plate (temperature 100 °C).

For the investigations of the influence of the sample shape on the fluorescence intensity 500 ng of arsenic (solution: 500 ppm, amount: 1 μL) were put on two different reflector materials (Si wafer and acrylic glass reflector). The preparation procedure was the same as described before except for the drying procedure (drying in vacuum). The use of different reflector materials led to different sample shapes.

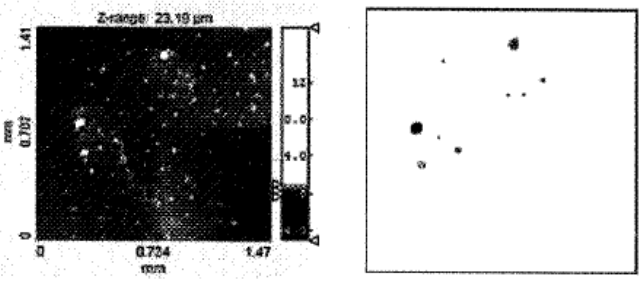

Figure 1. (Color online) 100 ng As before (left) and after (right) the speckle correction.

Vacuum drying is the more gentle drying procedure and since in this case the influence of the reflector material on the sample shape was investigated, this method was chosen to avoid a possible sample demolition by the drying procedure.

B. Analytical procedure

TXRF analysis was performed using two different systems to guarantee reproducibility: the ATOMIKA EXTRA-IIA system and the ATI TXRF vacuum chamber. The ATOMIKA EXTRA IIA system is equipped with a W and a Mo tube and a cut-off reflector. The measurements were done in Mo $K\alpha$ excitation mode at 1.27 mrad (angle of incidence), for 100 s live time, at 50 kV. The current was varied so that all measurements were done with the same dead time (40%). The ATI TXRF vacuum chamber is equipped with a Mo tube and a multilayer monochromator. The measurements were performed in Mo $K\alpha$ excitation mode at 70% of the critical angle ($\triangleq$1.25 mrad) (angle of incidence), for 500 s live time, at 40 kV and 10 mA.

C. Confocal microscopy

Measurements to determine the shape of the samples have been performed utilizing a confocal white light microscope [NanoFocus μsurf® (NanoFocus, Inc., 2009)]. The analyses were done by the Austrian Center of Competence for Tribology [AC2T (Austrian Center of Competence for Tribology (ACT), 2009)]. The measuring field was ~1450 $\times$1400 μm with a lateral resolution of ~1.5$\times$1.5 μm and 50 nm in height. Due to the measurement setup it was necessary to perform a plane correction. Furthermore speckles of questionable origin (traces of the sample, measurement artifacts, or contaminations), which were found on the quartz reflector surfaces have been removed by using a threshold filter. The threshold filter removed each data point with a height smaller than 10% of the maximum height of the sample. For further investigations it is recommended to inspect the reflectors for speckles before applying the samples. Figure 1 shows the 100 ng arsenic sample before and after the speckle correction.

III. THEORETICAL CONSIDERATIONS

A simulation model was developed to calculate the influence of the absorption effects. The model is applicable for the calculation of the fluorescence intensity emitted by a single-element sample in TXRF geometry. The base of the mathematical model is the formula for the calculation of the fluorescence intensity in XRF geometry given by Shiraiwa and Fujino, 1966 in the approximation for monoenergetic excitation. The following assumptions for the calculation were made:

- The detector is assumed to be ideal and covers the whole solid angle. So the geometry factors can be ignored and the detector efficiency is $\varepsilon=1$.
- The system is located in vacuum. Hence there is no absorption between tube and sample as well as sample and detector.
- The beam divergence is neglected.
- The fluorescence radiation is emitted perpendicular to the reflector surface.

To calculate the fluorescence intensity emitted by a sample of random shape in 2D the following approximation was made: any sample can be combined of n variably high (height h) and variably broad (width b) towers (Figure 2).

The calculation of the fluorescence intensity is done for any tower separately considering the attenuation of the primary intensity by the preceding towers. Furthermore it is necessary to make a case differentiation. There are three possible cases: the tower is hit by the beam (incident or reflected) completely (a), only partially (b), or not at all (c). The total intensity, which is emitted by the whole sample, results from a summation of the individual intensities. To obtain the fluorescence intensity emitted by a three-dimensional sample the intensity emitted by a tower is multiplied with its thickness. The points of impact of the primary

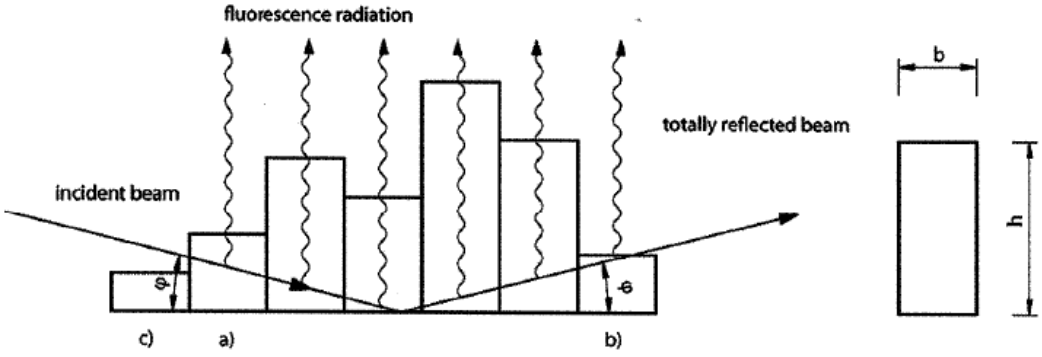

Figure 2. Schematic illustration of the towers geometry (2D).

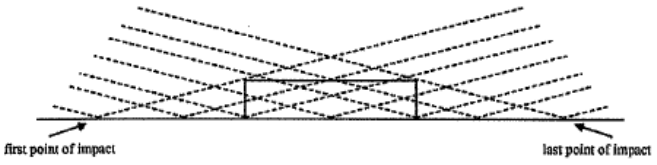

Figure 3. Selection of the points of impact.

radiation are selected so that the whole sample is illuminated (Figure 3). That means that the footprint of the system is bigger than the sample.

To accomplish an accurate calculation it is necessary to know all the parameters given in the formula. The sample dimensions and the volume were determined by analyses with a confocal white light microscope. The density of arsenic in the sample ρ_{real} was estimated from its dimensions (volume V_S) and mass (m_S):

$$\rho_{real} = m_S / V_S.$$

The values of the other fundamental parameters were obtained from databases (McMaster *et al.*, 1969; Krause, 1979; Scofield, 1974).

IV. RESULTS AND DISCUSSION

A. Linearity test

Figure 4 shows the results of the linearity test. With the Extra IIA system the samples were measured two times; the second time the samples were 90° rotated. The determination of the count rate of arsenic was accomplished with QXAS (Shiraiwa and Fujino, 1966). To compare the curve shapes the intensities (cps/mA) obtained by the Extra IIA system were divided by 2.75. During the measurements it was found that the relation between fluorescence intensity and sample amount is linear up to ~100 ng arsenic. At larger sample amounts deviations from the linearity occurred. The results of the measurements with the Extra IIA system show differences in the emitted intensities after rotating the samples. This could be caused either by a statistical error or an influence of the sample shape. The influence of the sample shape is discussed in the next part. The measured fluorescence intensity emitted by the samples was compared to the calculated intensity (Figure 5) to test the linearity of the calculations and the measurements. For the comparison the curves were normalized. The mean value of the quotients of the measured and calculated values was chosen as the normalization factor. However, the theoretical curve did not show

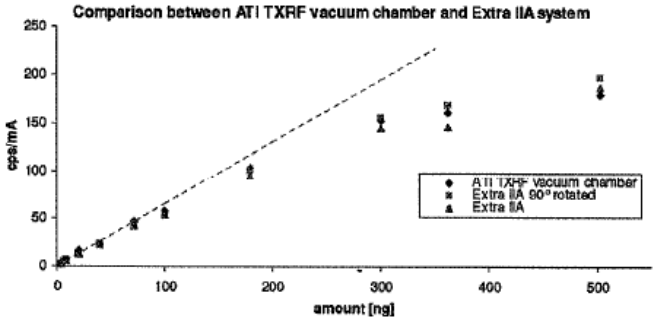

Figure 4. (Color online) Linearity test.

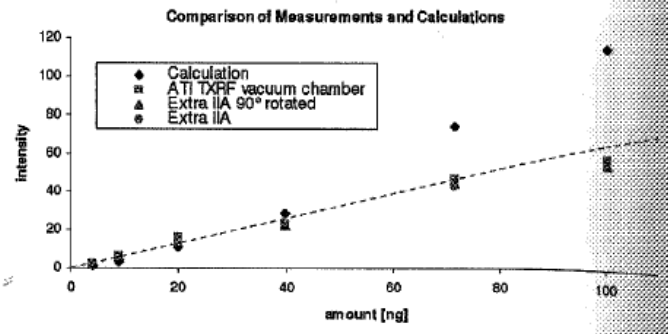

Figure 5. (Color online) Comparison of measurements and calculations.

the trend of the measured curve. Some of the difficulties for the simulation appear due to the determination of the density of arsenic in the sample. A possible error in the speckle correction could have led to a false value of the volume and hence of the density. Furthermore the samples do not contain pure arsenic but arsenic oxide. During the drying of the samples not all water is released (Holleman *et al.*, 1995). This could affect the density calculation more than expected. The result of the calculation for the 300 ng arsenic sample is not shown because the value of the intensity is much too high. The extension in x and y directions of this sample is four times larger than the extensions of the other samples and this could have led to a higher value of the calculated intensity.

B. Sample shape

The same sample amount of arsenic was put on a Si wafer and an acrylic glass reflector to investigate the resulting specimen shape. The drying of the samples led to different sample shapes. The sample dimensions were obtained by analyses with the confocal white light microscope. Figure 6 shows the plot of the sample on the acrylic glass reflector, which has a ring shape. Figure 7 shows the plot of the sample on the Si wafer. This sample is not ring shaped but tower-like formations shaped.

A theory for the formation of a ring by solids dispersed in a drying droplet is described by Deegan *et al.*, 2000b; Deegan, 2000a. According to this theory an outward flow within the droplet transports the solute to the contact line. (The contact line is the border where the surface of the droplet contacts the surface of the carrier.) This flow occurs when the contact line is pinned so that liquid which is removed by evaporation from the edge of the drop must be refilled by a flow of liquid from the inside. The reasons for the contact line pinning are irregularities of the substrate: surface roughness or chemical heterogeneity. Deegan *et al.* reported that no ring was formed when the pinning was eliminated by drying the drop on smooth Teflon. In this case the drying drop contracted as it dried. An expansion of the theory of Deegan was given by Popov, 2005 taking into account the volume occupied by the solute particles. Referring to the theory proposed by Deegan and Popov the formation of the residues could be explained as follows: some irregularity of the reflectors surface anchors the contact line of the deposited droplet at one or more points. As the liquid evaporates the solute particles are transported to these points and increase the pinning of the contact line. Eventually the primary

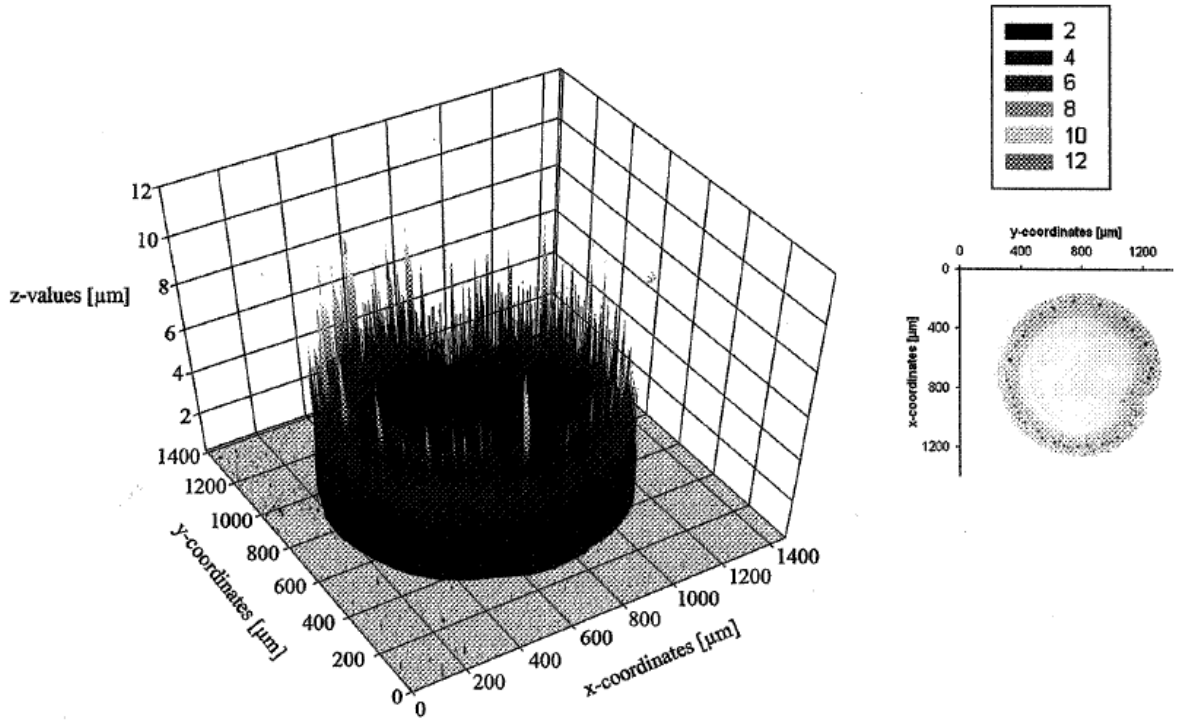

Figure 6. (Color online) Plot of the sample on the acrylic glass reflector.

droplet is disrupted to smaller droplets—one for each anchor point. Now these smaller droplets either undergo the same procedure again or contract at the anchor point. The shapes of the residues on the acrylic glass reflector and silicon reflector can be interpreted as antipodal extreme examples (Wobrauschek, 2007; Wobrauschek *et al.*, 1991). The surface of the silicon reflector has a very small roughness and is highly hygroscopic. Therefore the contact line could be pinned only at a few points and almost the whole primary droplet contracted at one point. The acrylic glass reflector has a higher surface roughness and is less hygroscopic. Hence the whole contact line of the primary droplet is pinned

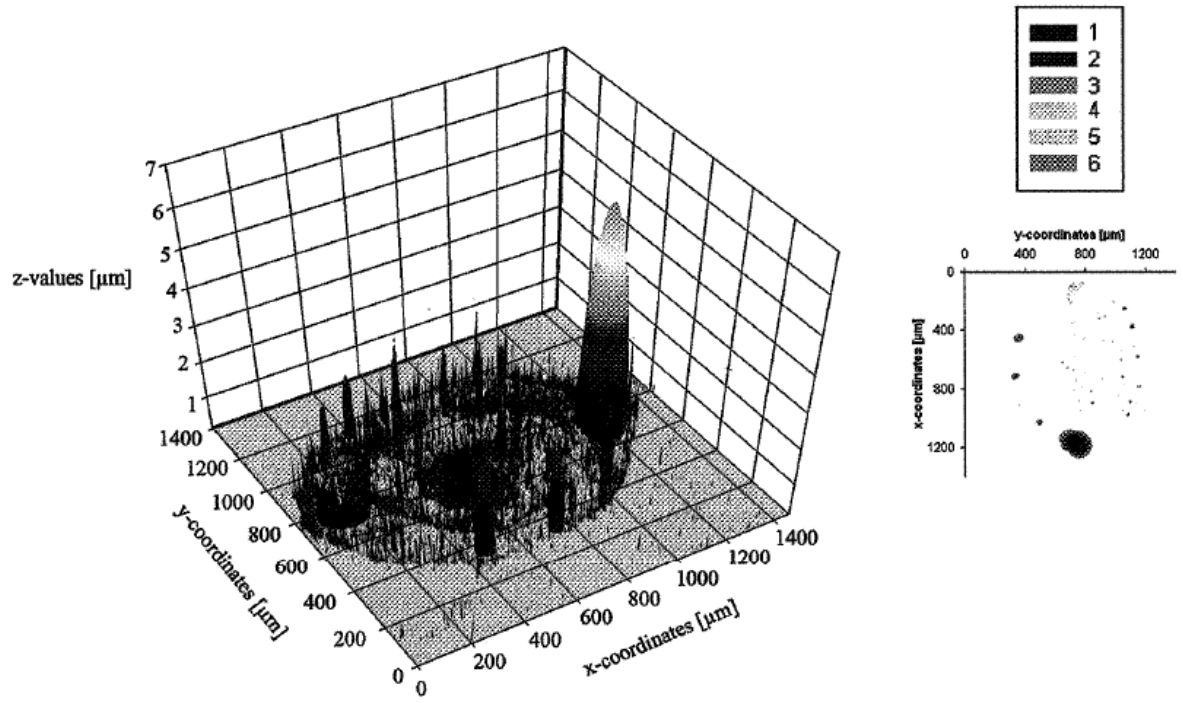

Figure 7. (Color online) Plot of the sample on the Si wafer.

TABLE I. Comparison of measured and calculated fluorescence intensities for different sample shapes.

	I/I0 (calculation) (%) scaled to maximum	I/I0 (measurement) (%) scaled to maximum
Si wafer	79	85
Acrylic glass reflector	100	100

at first. The solute particles are transported to the contact line and finally build a large number of small residues. Maybe this happens because they are themselves new anchor points.

C. Influence of the sample geometry

To investigate the influence of the sample geometry on absorption effects the fluorescence intensity emitted by the samples on the acrylic glass reflector and on the silicon reflector were measured and calculated. (Table I) Though the samples have different shapes, they have the same extensions in x and y directions and hence the same base. It was shown by both the calculation and the measurement that these differences of the sample shapes led only to minimal differing fluorescence intensities and hence that the influence of the sample shape for samples with the same base on the fluorescence intensity seems to be of less importance than expected. Assumption for the calculation: primary intensity $I0=1$.

V. CONCLUSIONS AND PERSPECTIVES

Presumably one of the key parameters for the absorption effect is the density of the investigated element in the dried residues. For further investigations it is necessary to find a better possibility for determining the real density of the sample. For example the way of crystallizing of the solution should be regarded in density calculations and the use of reflectors which are tested for speckles before applying the samples is recommended to avoid subsequent corrections. To confirm that the white light image is all based on the investigated element, μ-XRF measurements should be made to determine the actual elemental distribution.

Additionally the simulation model should be improved (e.g., consideration that the fluorescence intensity is emitted in all directions in space) and extended (to multielement samples and other geometries), respectively. Furthermore it was shown that the influence of the sample shape for samples with the same base on the fluorescence intensity seems to be of less importance. Now it has to be investigated if an influence of the sample geometry for samples with different extensions in x and y direction is negligible too. If the sample shape is influencing the intensity further investigations should include the following points:

- The sample preparation techniques have to be improved to obtain uniform dried spots. This would keep the influence of the sample geometry constant.
- The theoretically ideal TXRF specimen would be a thin, flat, homogeneous circle but especially at higher sample amounts it is almost impossible to produce. Further investigations will be done with picodroplet samples, which match the ideal form well. In this case it is possible to produce samples consisting of a pattern of picodroplets so that the whole sample amount is distributed on many small almost ideal TXRF samples.

Austrian Center of Competence for Tribology (ACT) (**2009**). (http://www.ac2t.at/), accessed 8 April 2009.

Deegan, R. D. (**2000a**). "Pattern formation in drying drops," Phys. Rev. E **61**, 475–485.

Deegan, R. D., Bakajin, O., Dupont, T. F., Huber, G., Nagel, S. R., and Witten, T. A. (**2000b**). "Contact line deposits in an evaporating drop," Phys. Rev. E **62**, 756–765.

Fabry, L. and Pahlke, S. (**2002**). *Surface and Thin Film Analysis*, edited by Bubert, H. and Jenett, H. (Wiley, Weinheim), pp. 181–193.

Hellin, D., Fyen, W., Rip, J., Delande, T., Mertens, P. W., Gendt, S. D., and Vinckier, C. (**2004a**). "Saturation effects in TXRF on micro-droplet residue samples," J. Anal. At. Spectrom. **19**, 1517–1523.

Hellin, D., Rip, J., Arnauts, S., De Gendt, S., Mertens, P. W., and Vinckier, C. (**2004b**). "Validation of vapor phase decomposition–droplet collection–total reflection X-ray fluorescence spectrometry for metallic contamination analysis of silicon wafers," Spectrochim. Acta, B At. Spectrosc. **59**, 1149–1157.

Hellin, D., Rip, J., Geens, V., Delande, T., Conard, T., Gendt, S. D., and Vinckier, C. (**2005**). "Remediation for TXRF saturation effects on microdroplet residues from preconcentration methods on semiconductor wafers," J. Anal. At. Spectrom. **20**, 652–658.

Holleman, A. F., Wiberg, E., and Wiberg, N. (**1995**). *Lehrbuch der Anorganischen Chemie* (Walter de Gruyter, New York), p. 2033.

IAEA (**1995**). *QXAS, AXIL Version* (IAEA, Vienna).

Klockenkämper, R. (**1996**). *Total Reflection X-ray Fluorescence Analysis* (Wiley, Weinheim).

Krause, M. O. (**1979**). "Atomic radiative and radiationless yields for K and L shells," J. Phys. Chem. Ref. Data **8**, 307–327.

Kregsamer, P., Streli, C., and Wobrauschek, P. (**2001**). *Handbook of X-ray Spectrometry*, edited by Van Grieken, R. and Markowicz, A. (Marcel Dekker, New York), pp. 559–602.

Ladisich, W., Rieder, R., Wobrauschek, P., and Aiginger, H. (**1993**). "Total reflection X-ray fluorescence analysis with monoenergetic excitation and full spectrum excitation using rotating anode X-ray tubes," Nucl. Instrum. Methods Phys. Res. A **330**, 501–506.

McMaster, W. H., Del Grande, N. K., Mallett, J. H., and Hubbell, J. H. (**1969**). Compilation of X-Ray Cross Sections, Section II Revision I (Report No. UCRL-50174). Livermore, CA: Lawrence Livermore National Laboratory.

NanoFocus, Inc. (**2009**). (http://www.nanofocus.de/usurf-explorer.html?&L=1), accessed 8 April 2009.

Pahlke, S. (**2003**). "Quo Vadis total reflection X-ray fluorescence?" Spectrochim. Acta, B At. Spectrosc. **58**, 2025–2038.

Pahlke, S., Fabry, L., Kotz, L., Mantler, C., and Ehmann, T. (**2001**). "Determination of ultra trace contaminants on silicon wafer surfaces using total-reflection X-ray fluorescence TXRF 'state-of-the-art'," Spectrochim. Acta, B At. Spectrosc. **56**, 2261–2274.

Popov, Y. O. (**2005**). "Evaporative deposition patterns: Spatial dimensions of the deposit," Phys. Rev. E **71**, 1-17.

Prange, A. and Schwenke, H. (**1992**). "Trace element analysis using total-reflection X-ray fluorescence spectrometry," Adv. X-Ray Anal. **35**, 899–923.

Scofield, J. A. (**1974**). "Exchange corrections of K x-ray emission rates," Adv. At., Mol., Opt. Phys. **9**, 1041–1049.

Shiraiwa, T. and Fujino, N. (**1966**). "Theoretical calculation of fluorescent X-ray intensity in fluorescent x-ray petrochemical analysis Japan," Jpn. J. Appl. Phys. **5**, 886–899.

Stoev, K. N. and Sakurai, K. (**1999**). "Review on grazing incidence X-ray spectrometry and reflectometry," Spectrochim. Acta, B At. Spectrosc. **54**, 41–82.

Wobrauschek, P. (**2007**). "Total reflection x-ray fluorescence analysis—a review," XRay Spectrom. **36**, 289–300.

Wobrauschek, P., Kregsamer, P., Streli, C., and Aiginger, H. (**1991**). "Recent developments and results in total reflection X-ray fluorescence analysis," Adv. X-Ray Anal. **34**, 1–12.

Wobrauschek, P., Kregsamer, P., Streli, C., Rieder, R., and Aiginger, H. (**1992**). "TXRF with various excitation sources," Adv. X-Ray Anal. **35**, 925–931.